LETTERS
PUBLISHED ONLINE: 28 JULY 2013 | DOI: 10.1038/NNANO.2013.142
nature nanotechnology

Autonomous molecular cascades for evaluation of cell surfaces

Maria Rudchenko[1†], Steven Taylor[1†], Payal Pallavi[2], Alesia Dechkovskaia[1], Safana Khan[2], Vincent P. Butler Jr[2], Sergei Rudchenko[1,2*] and Milan N. Stojanovic[2,3*]

Molecular automata are mixtures of molecules that undergo precisely defined structural changes in response to sequential interactions with inputs[1-4]. Previously studied nucleic acid-based automata include game-playing molecular devices (MAYA automata[3,5]) and finite-state automata for the analysis of nucleic acids[6], with the latter inspiring circuits for the analysis of RNA species inside cells[7,8]. Here, we describe automata based on strand-displacement[9,10] cascades directed by antibodies that can analyse cells by using their surface markers as inputs. The final output of a molecular automaton that successfully completes its analysis is the presence of a unique molecular tag on the cell surface of a specific subpopulation of lymphocytes within human blood cells.

The problem of labelling a narrow subpopulation of cells within a much larger population of related cells is often faced, because of the need to specifically tag a particular cell type for the purpose of elimination[11], analysis and isolation[12], or imaging[13]. This challenge could be readily addressed in a direct manner if targeted subpopulations could have some unique cell-surface marker[13] against which antibodies could be raised. However, as exemplified by a cancer therapy utilizing antibody–drug conjugates (ADCs), markers are often shared by non-targeted cells, leading, in this case, to off-target toxicities[13]. To uniquely target cells that have no distinctive markers on their surfaces, we need to use a set of multiple markers for each subpopulation in a Boolean manner. Molecular automata that undergo structural changes ('state transitions') coupled to the sequential recognition of a selected set of cell surface markers might be able to contract the set into a single tag and thus provide a unique handle for the targeted cells. In other words, in the language of molecular computing[14,15], these molecular devices would autonomously (that is, without any human participation) evaluate Boolean functions on cell surfaces, with surface markers as inputs and a tag as an output.

We chose to utilize blood cells as the targets for molecular automata, because these cells are the most exhaustively studied[16], with lineages and stages of differentiation defined by the presence or absence of multiple cell-surface markers. They are commonly characterized using flow cytometry according to their different levels of expression of multiple cell surface markers[14], known as 'clusters of differentiation' (CDs). In this work we use CD45, CD20, CD3 and CD8 as examples. Figure 1 presents the basic design principles for automata that will tag lymphocytes with targeted CD markers characteristic of B cells, that is, $CD45^+CD20^+$ cells, in the presence of non-targeted $CD45^+CD20^-$ cells (for example, $CD45^+CD3^+$, T cells).

The exact 'program' (that is, conditional sequential transitions) that the automata will execute on the surfaces of the lymphocytes will be defined by sets of antibodies against CD markers M_i, which direct the cascade (see Fig. 1, with CD45 and CD20 as M_i). We started with the well-established off-the-shelf antibodies targeting CD markers: αCD45, αCD45RA, αCD20 (Rituximab), αCD3 and αCD8. All these antigens are present at a level of 80,000–200,000 copies per cell surface on targeted subpopulations of lymphocytes, ensuring a strong signal when measured by flow cytometry. These antibodies were conjugated[17] with a set of partially complementary oligonucleotides (**1·2**, **3·4** and **5·6**) optimized to execute modified strand-displacement cascades[9] when triggered with oligonucleotide **0** (Fig. 1b,c; Supplementary Figs S1–S6). Once turned on, the automata based on these antibody conjugates will perform 'if YESM_i then proceed' or 'if NOTM_i then proceed' assessments of M_i markers on the surface of individual cells via oligonucleotide transfers enabled by sequential exposure of new toeholds (Fig. 1b) and driven by the formation of oligonucleotide duplexes with more complementarity (**0·1**, **2·3** and **4·5**).

The first step in demonstrating the performance of the automata is to test their ability to evaluate two surface markers (see Fig. 2a for the YESCD45YESCD20 experiment, functionally equivalent to the Boolean CD45ANDCD20) and to selectively label one targeted subpopulation within a population of peripheral blood mononuclear cells (PBMCs). We constructed all possible automata that could assess combinations of two out of three markers, CD45 (a marker of nucleated haematopoietic cells), CD20 (a B-cell marker) and CD3 (a pan-T-cell marker). Two of the automata are capable of successfully completing their program: YESCD45YESCD20 would operate (label) only on B cells (Fig. 2a) and YESCD45YESCD3 would operate only on T cells (Supplementary Fig. S7). The third possible two-step automaton, YESCD3YESCD20, is a negative control, because no subpopulation displays these two markers at the same time (Supplementary Fig. S7c). Operation of these automata is equivalent to asking 'Is this cell a nucleated haematopoietic cell?' (YESCD45) followed by, in the case of the first automaton, 'Is this a nucleated haematopoietic cell from a B-cell lineage?' (YESCD20), and, in the case of the second automaton, 'Is this nucleated haematopoietic cell from the T-cell lineage?' (YESCD3). In all these automata, if both questions are answered positively consecutively, the reaction performed (on B cells, as an example) will be $\mathbf{0} + \mathbf{1{\cdot}2}_{\alpha CD45} + \mathbf{3{\cdot}4}_{\alpha CD20} \rightarrow \mathbf{0{\cdot}1} + {}_{\alpha CD45}\mathbf{2{\cdot}3} + {}_{\alpha CD20}\mathbf{4}$, with targeted subpopulations displaying a newly uncovered single-stranded oligonucleotide, **4**. This one marker then contains the same information as traditional multicolour labelling, but with the same antibodies that we used in the construction of the automata and that we would otherwise use to characterize the immunological phenotype of these cells (for example, as $CD45^+CD20^+$). We also set up a

[1]Research Division, Hospital for Special Surgery, 535E 70th Street, New York 10021, New York, USA, [2]Department of Medicine, Columbia University, 630W 168th Street, New York, New York 10032, USA, [3]Departments of Biomedical Engineering and Systems Biology, Columbia University, 630W 168th Street, New York, New York 10032, USA, †These authors contributed equally to this work. *e-mail: rudchenkoS@hss.edu; mns18@columbia.edu

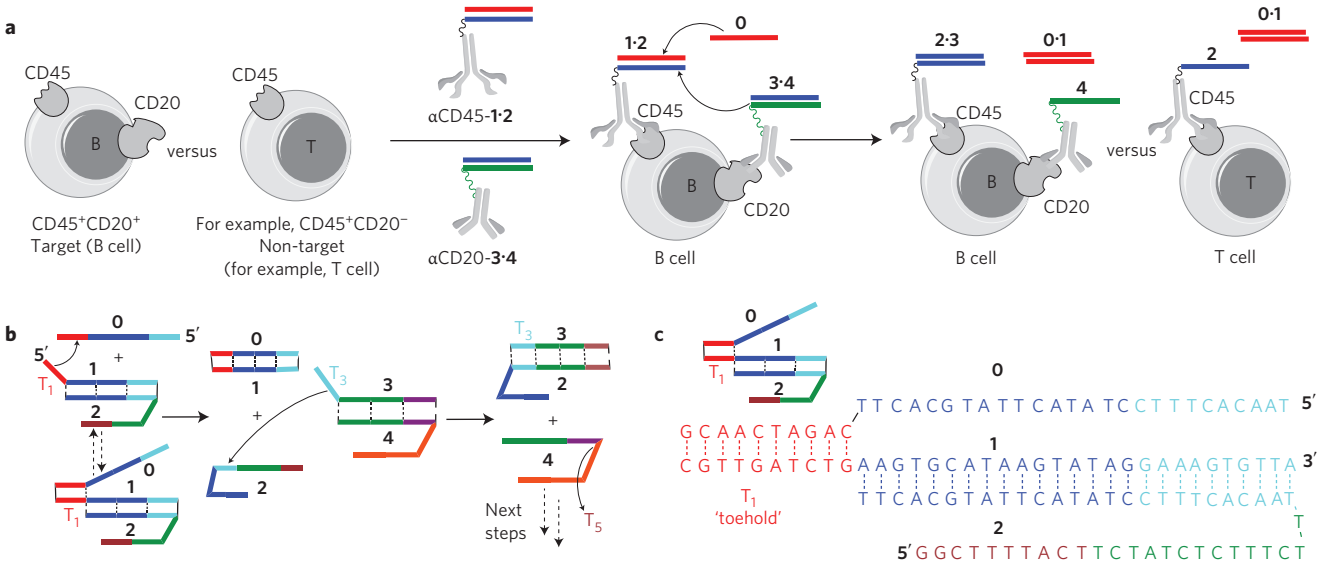

Figure 1 | Design considerations for automata operating on cell surfaces. a, Scheme of automata operating on a B cell with a $C45^{+}CD20^{+}$ phenotype (target) and on an example of a non-targeted cell with a $CD45^{+}CD20^{-}$ phenotype (for example, a T cell). Oligonucleotide components (coloured horizontal lines) attached to antibodies (Y-shaped structures) are brought together on some cells and not others (for example, αCD45-**1·2** and αCD20-**3·4** are together only on B cells), leading to a cascade of oligonucleotide transfers driven by an increase in complementarity. The transfers result in a unique single-stranded oligonucleotide **4** being displayed only on targeted cells. **b**, Scheme of a typical strand displacement reaction used in the automata $\mathbf{0} + \mathbf{1{\cdot}2} + \mathbf{3{\cdot}4} \rightarrow \mathbf{0{\cdot}1} + \mathbf{2{\cdot}3} + \mathbf{4}$, controlled by a sequential exposure of toeholds (T_1 then T_3): single-stranded oligonucleotide **0** displaces oligonucleotide **2** from its complex with **1** via toehold interactions, that is, stronger complementarity and kinetic enablement due to the additional complementarity with exposed T_1. This generates an oligonucleotide stretch in strand **2** complementary to a toehold T_3 in strand **3** that can extend the reaction cascade by displacing oligonucleotide **4** from **3·4**. This in turn generates the next oligonucleotide stretch complementary to toehold T_5, which can be used to extend the cascade to **5·6** (not shown), and so on (as indicated by double dotted arrows), or to label the cell with **5** carrying fluorescein. Without other components displaying T_5, the cascade stops at **4**. **c**, An example of oligonucleotide sequences used in the automata. Complete oligonucleotide sequences are available in Supplementary Fig. S1.

system so that the output oligonucleotide (**4**) would interact with a solution-phase label as in $_{\alpha CD20}\mathbf{4} + \mathbf{5{\cdot}6} \rightarrow {}_{\alpha CD20}\mathbf{4{\cdot}5} + \mathbf{6}$ (where **5** is labelled with fluorescein), thus allowing direct analysis by flow cytometry of the response of targeted cells within a heterogeneous population of cells to the cascade. To assess the full operation of the automata, we labelled **1** with Cy5, so both its removal and subsequent acquisition of fluorescein by $_{\alpha CD20}\mathbf{4}$, on the cell surface, could be monitored simultaneously in real time.

In our experiments, the first two automata successfully labelled only the surfaces of either B ($CD45^{+}CD20^{+}$) or T ($CD45^{+}CD3^{+}$) cells (Fig. 2a,b; Supplementary Figs S7 and S8), with each outcome confirmed three or more times on individual human blood samples and monitored by multicolour flow cytometry. From these same components we also constructed an automaton that could label the surfaces of both B and T cells by using $\mathbf{3{\cdot}4}_{\alpha CD20}$ and $\mathbf{3{\cdot}4}_{\alpha CD3}$ in the same solution (see Supplementary Fig. S7e). A possible presentation of this automaton is as an OR function, as in YESCD45(YESCD20ORYESCD3). In control experiments, we also confirmed that the automata worked on enriched cell subpopulations with the correct marker combinations (B or T cells, see Supplementary Fig. S8).

We next studied negative controls in more detail, that is, antibody-directed cascades that can occur only between markers on separate cells (between two subpopulations). Using the third possible two-step automaton introduced above, YESCD3YESCD20, we observed no labelling within the timeframe of our experiment, indicating that the T cells did not visibly exchange elements with B cells, either through diffusion or through direct physical contact of cells (Supplementary Fig. S9). We also separated T and B cells, labelling the former with $\mathbf{1{\cdot}2}_{-\alpha CD3}$ and the latter with $\mathbf{3{\cdot}4}_{-\alpha CD20}$. Upon remixing the cells, we observed no crosstalk between the different lineages, within the detection limits of the flow cytometer (Supplementary Fig. S9). Finally, we demonstrated that automata YESCD20YESCD45, with an inverted order of assessing the cell, worked without labelling any $CD45^{+}CD20^{-}$ cells (Supplementary Fig. S10). All these experiments demonstrate low noise in the automata in the absence of an excess of elements in the solution phase (that is, they demonstrate minimal tagging of cells via diffusion or by direct contact between cells). To estimate the effects of washing away excess antibody conjugates, we studied automata YESCD3YESCD20 and YESCD3(YESCD20ORYESCD8) without prior removal of excess components from the solution. In both cases we observed changes in the fluorescence of non-targeted cells, albeit several-fold weaker than in targeted cells (Supplementary Fig. S9), indicating that proximity-based interactions on a single cell were dominant.

The structures comprising these two-step automata were adjusted to enable cells to be labelled with fluorescent oligonucleotides only in the absence of a CD marker, that is, an 'if NOTM_i then proceed' function (NOTM_i, Fig. 3, Supplementary Fig. S11). During the differentiation of T cells, from naive to memory, there is a transition in the expression of two different isoforms of CD45 (CD45RA and CD45RO), so we created an automaton to assess the presence of isoforms of CD45 on $CD8^{+}$ T cells, with the CD45RA isoform inhibiting the cascade. The automaton YESCD8NOTCD45RA consisted of $\mathbf{3{\cdot}4}_{\alpha CD8}$ and $\mathbf{5^{*}{\cdot}6^{*}}_{\alpha CD45RA}$ triggered by **2** in the presence of solution-phase **5·6** (where **5** is labelled with fluorescein). All cells that responded to the automaton and acquired **5** from the solution phase strongly expressed CD45RO; that is, these were $CD45RA^{-}$ cells (Fig. 3b, Supplementary Fig. S11b). This was in contrast to the $CD8^{+}CD45RA^{+}$ T cells (namely $CD45RO^{-}$ or $CD45RO^{dim}$), which were hindered in

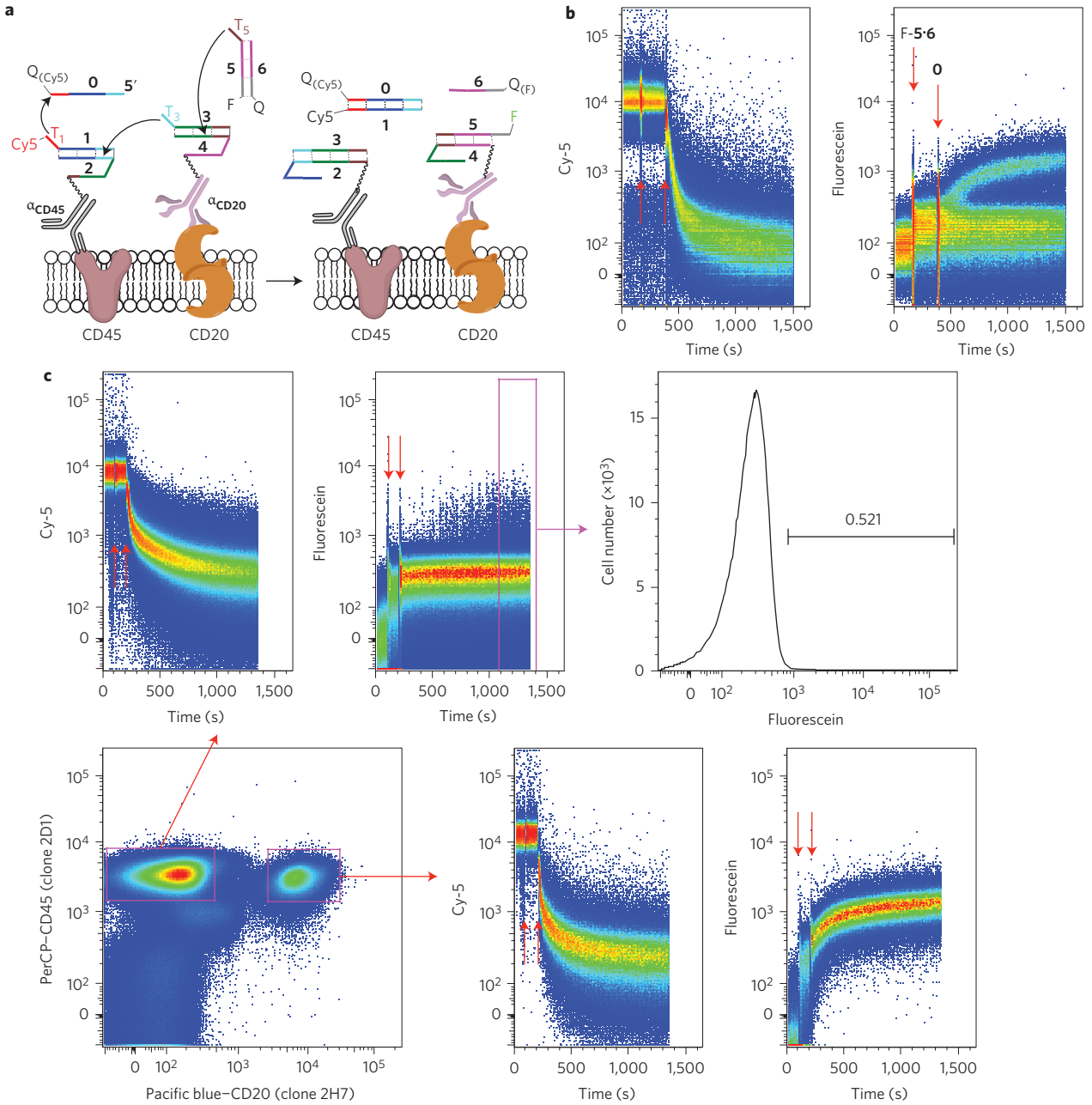

Figure 2 | Demonstration of automata assessing the presence of two cell-surface markers. a, Scheme of YESCD45YESCD20 automata implementing reaction cascade **0** + **1·2**$_{\alpha CD45}$ + **3·4**$_{\alpha CD20}$ + **5·6** → **0·1** + $_{\alpha CD45}$**2·3** + $_{\alpha CD20}$**4·5** + **6** on the cell surface. **1** is labelled with Cy5 and **0** with a quencher (Q_{Cy5}, Iowa Black RQ) for Cy5; **5** is labelled with fluorescein (F), and **6** is labelled with a quencher (Q_F, Iowa Black FQ) for fluorescein. **b**, Flow cytometry monitoring of the YESCD45YESCD20 cascade (each dot represents the fluorescence signal level from a single cell at the time of measurement, with dot density representing the number of cells, shown as increasing from blue to red). Time course of the cascade reaction on $CD20^+$ B cells: (left) monitoring the removal of Cy5-**1** occurring on $CD45^+$ cells after the triggering reaction with **0**; (right) fluorescein-labelled **5** is taken up from solution by $CD20^+$ B cells, which is used for monitoring the acquisition of **5** by **4** enabled by prior removal of **3** from **4**. The addition of **5·6** (indicated by the first red arrow) produces an immediate fluorescence increase on all cells due to incomplete quenching of fluorescein. The addition of **0** (indicated by the second red arrow) triggers the cascade and separation of the subpopulations of cells. **c**, Monitoring of a cascade on individual subpopulations within PBMCs using fluorescently labelled monoclonal antibodies targeting the same CDs but different non-overlapping epitopes for identification of cell subpopulations (PerCP–CD45 antibody, clone 2D1 and Pacific Blue–CD20 antibody, clone 2H7). These results confirm that all $CD45^+CD20^+$ cells (right gate, that is, the right box in the bottom left panel) are labelled by automata (that is, there is an increase in fluorescein uptake from solution, see bottom middle and right panels) and that cells that are $CD45^+CD20^-$ (left gate, that is, left box in the bottom left panel) are not (upper left and central panels). It is seen that ~0.5% of the cells that are gated (box in the middle top panel) as $CD45^+CD20^-$ may react with a delay (top right panel). Red arrows have the same meaning as in **b**.

acquiring **5** due to competition with **5*** from the CD45RA in proximity to CD8-displaying **4**, instead forming **5*·4**$_{\alpha CD8}$ (Fig. 3, Supplementary Fig. S11). It should be noted that the 'if NOTM_i then proceed' function is limited, until a threshold[9] function is introduced, by the ratio of levels of expression of individual markers on the cell surface.

At this point, we have established three types of transition that could be used to build larger automata, YESM_i, NOTM_i and OR (the

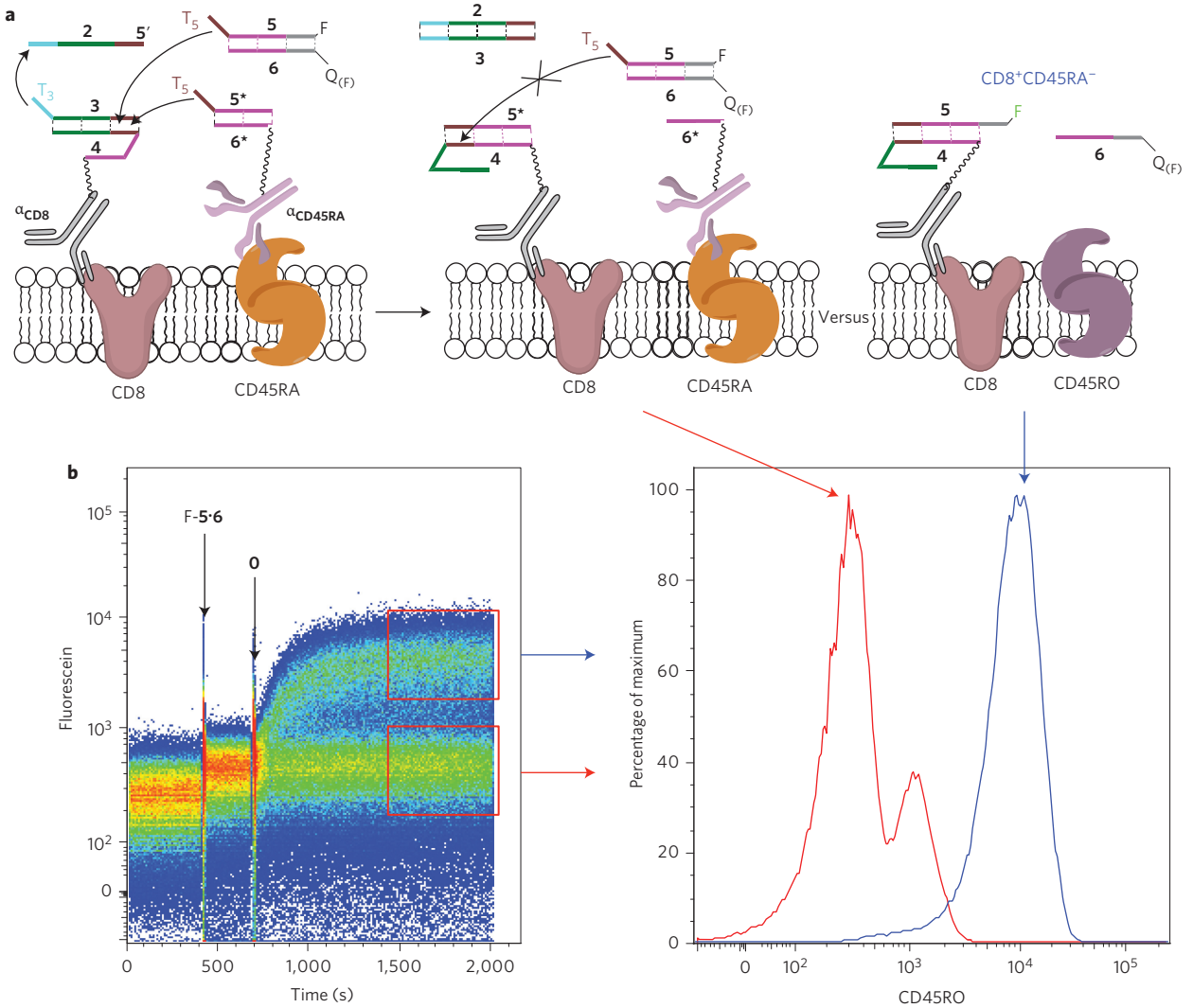

Figure 3 | Demonstration of automata assessing the absence of a cell-surface marker. a, Scheme of a YESCD8NOTCD45RA cascade protecting naive $CD8^+CD45RA^+$ T cells. In these cells, the CD45RA isoform prevents the targeting of CD8. This automaton works by: if cell is CD8 positive and if cell is CD45RA positive (or $CD45RO^{neg}$) then reaction is $\mathbf{2} + \mathbf{3{\cdot}4}_{\alpha CD8} + \mathbf{5^*{\cdot}6^*}_{\alpha CD45RA} + \mathbf{5{\cdot}6} \rightarrow \mathbf{2{\cdot}3} + \mathbf{5^*{\cdot}4}_{\alpha CD8} + \mathbf{6^*}_{\alpha CD45RA} + \mathbf{5{\cdot}6}$, resulting in no labelling (red trace in right panel of **b**), else, when cell is $CD45RA^-$ (CD45RO isoform), the reaction is $\mathbf{2} + \mathbf{3{\cdot}4}_{\alpha CD8} + \mathbf{5{\cdot}6} \rightarrow \mathbf{2{\cdot}3} + \mathbf{5{\cdot}4}_{\alpha CD8} + \mathbf{6}$; as a result, fluorescein-labelled **5** is removed from quencher (Q_F, Iowa Black FQ) strand **6** and is taken up from the solution in a simple YESCD8 response (blue trace in right panel of **b**). **b**, Monitoring of the YESCD8NOTCD45RA cascade. Left: time course of the cascade reaction on the surface of $CD8^+$ T cells from peripheral blood. Right: histograms (or frequency distributions) of memory $CD8^+$ T cells responding to automata (upper gate/box in left panel; blue trace in right panel, $CD8^+CD45RO^+$ or $CD45RA^-$) while naive $CD8^+$ T cells are being protected from the automaton (lower gate/box in left panel; red trace, $CD8^+CD45RO^-/CD45RA^+$). For gating strategy, see Supplementary Fig. S11.

last function consisting of adding to the cells two antibodies conjugated to identical oligonucleotide components). As an example of the feasibility of building more complex automata from these simple transitions, we proceeded to build an automaton with a three-step cascade, evaluating the presence of up to three markers, and executing YESCD45YESCD3YESCD8 on the cell surface (the third question is 'Is this nucleated haematopoietic cell of T cell lineage a CD8 positive cell?'). In this automaton, the surface of $CD8^+$ cells enabled the following reaction: $\mathbf{0} + \mathbf{1{\cdot}2}_{\alpha CD45} + \mathbf{3{\cdot}4}_{\alpha CD3} + \mathbf{5{\cdot}6}_{\alpha CD8} + \mathbf{7{\cdot}8} \rightarrow \mathbf{0{\cdot}1} + {}_{\alpha CD45}\mathbf{2{\cdot}3} + {}_{\alpha CD3}\mathbf{4{\cdot}5} + {}_{\alpha CD8}\mathbf{6{\cdot}7} + \mathbf{8}$. The labelling scheme allowed us to monitor each step in this cascade, via flow cytometry, in real time (Fig. 4,b, Supplementary Fig. S12). This automaton was successfully demonstrated on targeted cells, with changes in the fluorescence of cells being consistent with changes in the distances between various components at each step of the cascade (the first step is monitored by the removal of Pacific Blue, the second by the drop in Cy5 due to quenching, and the third by the acquisition of fluorescein from solution).

Finally, we tested our automata under conditions that could lead to the development of applications. First, we were able to demonstrate that we could isolate (with a purity equivalent to a standard isolation protocol) fluorescein-labelled cells with a YESCD45YESCD3 automaton. For this, we used a standard method for the isolation of cells (Fig. 5a, using anti-fluorescein antibody conjugated to magnetic beads). Second, we were able to demonstrate that an automaton (we used YESCD3YESCD8) can function in whole blood. For this, we could simply add the automata components to the mixture, all together, before triggering the reaction (Fig. 5b). The first demonstration is important, because it shows that there is no detectable decrease in the purity of isolated cells achieved using a single-step automaton-based procedure (*in situ* cascade) when compared to a standard separation protocol based on

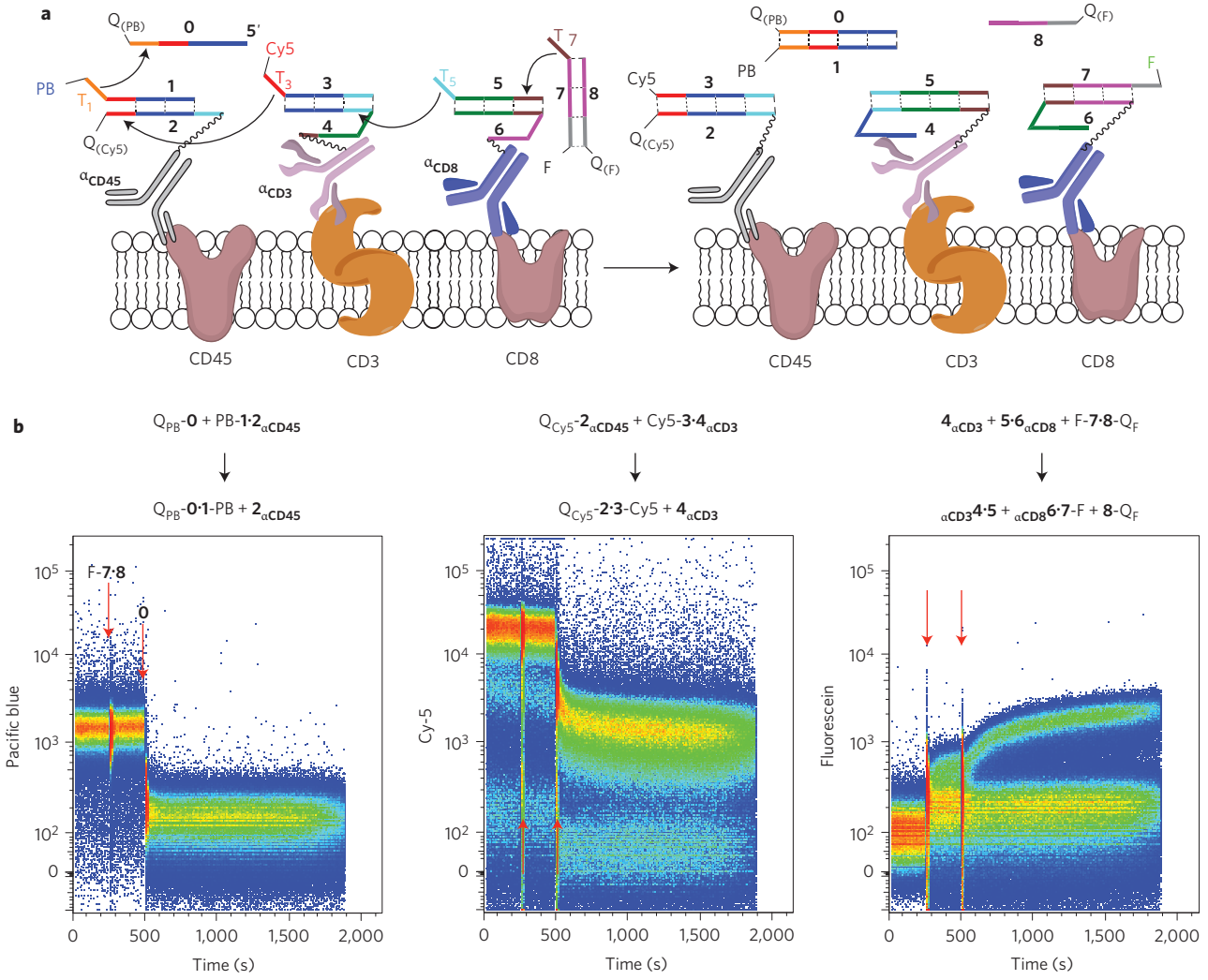

Figure 4 | Demonstration of automata assessing the presence of three markers (CD45, CD3 and CD8) on the surface of the cell. a, Scheme of a YESCD45YESCD3YESCD8 cascade (individual antibody conjugates: α_{CD45} with **1·2** complex, α_{CD3} with **3·4** and α_{CD8} with **5·6**). Oligonucleotides are labelled with fluorescent dyes and quenchers to facilitate monitoring of multiple events in parallel (**1** with Pacific Blue (PB), **3** with Cy5, **7** with fluorescein (F); **0** with a quencher ($Q_{(PB)}$, Iowa Black FQ) for Pacific Blue, **2** with a quencher ($Q_{(Cy5)}$, Iowa Black RQ) for Cy5, and **8** with a quencher ($Q_{(F)}$, Iowa Black FQ) for fluorescein). **b**, Flow cytometry monitoring in three colours of the state transition (*y*-axis, fluorescence intensity; *x*-axis, time; arrows show events, such as the additions of oligonucleotides **7·8** and **0**). Left: the first step, with Pacific Blue removed from the cell surface by **0**. Middle: the second step, transfer of **3** to **2**, by quenching of Cy5. Right: the third step, not observed directly, is the transfer of **5** to **4**, but by the uptake of **7** from a solution by **6**. In the final step (right, fluorescein), the separation of $CD45^+CD3^+CD8^+$ from all other lymphocytes is clearly shown.

individual separation steps for each CD marker. The second experiment also established that blood components do not interfere with the cascades. Together with demonstrations that interactions via solution-phase information transfer do not represent major pathways in labelling cells (*vide supra* and Supplementary Fig. S9), this experiment opens up the possibility of using automata for labelling and eventually eliminating cells *in vivo*, depending on the pharmacokinetic properties of our conjugates.

In conclusion, we have established that a combination of antibodies and oligonucleotide-based reaction cascades can operate as molecular automata to assess the presence or absence of cell surface markers on living human cells. These results extend the use of molecular automata beyond analysis by transfecting oligonucleotides into cells[7,8], thereby permitting new operations on the surfaces of native cells. Unlike previous utilizations of proximity principles such as bispecific antibodies[18] or proximity ligation reactions[19], our approach can be readily expanded to more complex logic operations and to the protection of cells through a NOT transition. The demonstrated systems also contribute to the emerging field of molecular robotics[20–22]. One approach to cell analysis with molecular robots is to increase the complexity of individual nanoparticles using the self-assembly of DNA nanoobjects displaying multiple aptameric locks[22]. Here, we offer an alternative and potentially simpler method, in which we use a number of elementary components that are brought together by the cell surface to execute more complex programmable (automata) functions, an approach that is conceptually similar to that of the distributed robotics paradigms[23].

Methods

Detailed protocols, all sequences and their optimization, and full characterization of all synthesized reagents are provided in the Supplementary Information. Briefly, oligonucleotides were coupled to antibodies, unless stated otherwise, in a two-step procedure: (i) dithiothreitol (DTT) was used under conditions that reduce interchain disulphide bonds; (ii) 5′-end maleimide-functionalized oligonucleotides were coupled to the reduced antibody sulfhydryls, and the products were purified using gel filtration. One biotinylated antibody was used in the NOTCD45RA cascade, with streptavidin used to crosslink it to biotinylated oligonucleotides. This procedure was performed directly on cells without purification of conjugates (in this case, negative controls with no streptavidin and no antibody were also successfully run). Reagents

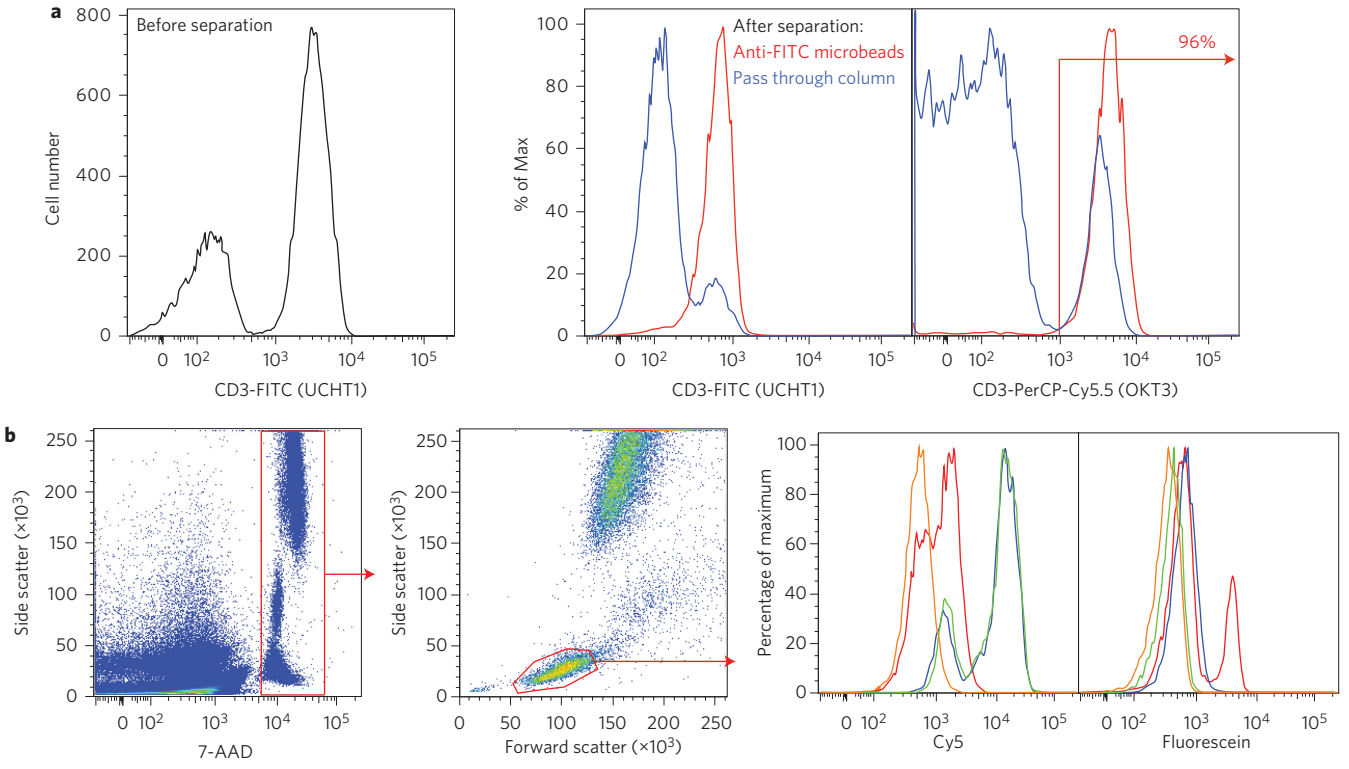

Figure 5 | Demonstrations of the potential for practical applications. a, Magnetic separation of $CD3^+$ cells from PBMCs based on the results of a YESCD45YESCD3 automaton. Before the cascade (left), we see a mixture of cells with different $CD3^+$ status. After the cascade, cells were incubated with magnetic microbeads conjugated with anti-FITC antibodies (Miltenyi Biotec) and applied on a MACS Column (Miltenyi Biotec; purity of the post-isolation preparation was >95%). The 'pass-through' fraction (blue line in middle panel) and the magnetically labelled cells (red line in middle panel) were re-analysed with different clones of αCD3 antibodies (that is, different epitopes of the same CD) to confirm purity (right). **b**, YESCD3YESCD8 automaton examined in whole blood. Left and middle: flow cytometry analysis with gating strategy. Nucleated cells are gated by staining their DNA with 7-AAD, with lymphocytes selected based on forward and side scatter. The histograms show end points of two steps of the cascade as performed in blood. Cy5 fluorescence is used to show that the first step has been accomplished, and fluorescein is used to demonstrate that the second step has been accomplished, as in Fig. 2). Lines on histograms: yellow, unlabelled blood sample; green, blood sample incubated for 15 min with αCD3 conjugated with duplex **1·2** and αCD8 conjugated with duplex **3·4**; blue, same, but with **5·6** added and also incubated for 15 min; red, subsequent addition of **0** after incubation for 15 min.

were added to cell suspensions, and in all experiments involving PBMCs, reagents were removed from solution by centrifugation. In whole-blood experiments (Fig. 5), reagents were left in blood to mimic the conditions for potential *in vivo* applications.

Received 3 December 2012; accepted 19 June 2013; published online 28 July 2013

References

1. Rothemund, P. in *1st DIMACS Workshop on DNA Based Computers* (eds Lipton, R. J. & Baum, E. B.) 75–120 DIMACS Series 27 (American Mathematical Society, 1996).
2. Benenson, Y. *et al.* Programmable and autonomous computing machine made of biomolecules. *Nature* **414,** 430–434 (2001).
3. Stojanovic, M. N. & Stefanovic, D. A deoxyribozyme-based molecular automaton. *Nature Biotechnol.* **21,** 1069–1074 (2003).
4. Wang, Z.-G., Elbaz, J., Remacle, F., Levine, R. D. & Willner, I. All DNA finite-state automata with finite memory. *Proc. Natl Acad. Sci. USA* **107,** 21996–22001 (2010).
5. Pei, R., Matamoros, E., Liu, M., Stefanovic, D. & Stojanovic, M. N. Training a molecular automaton to play a game. *Nature Nanotech.* **5,** 773–777 (2010).
6. Benenson, Y., Gil, B., Ben-Dor, U., Adar, R. & Shapiro, E. An autonomous molecular computer for logical control of gene expression. *Nature* **429,** 423–429 (2004).
7. Rinaudo, K. *et al.* A universal RNAi based logic evaluator that operates in mammalian cells. *Nature Biotechnol.* **25,** 795–801 (2007).
8. Xie, Z., Wroblewska, L., Prochazka, L., Weiss, R. & Benenson, Y. Multi-input RNAi-based logic circuit for identification of specific cancer cells. *Science* **333,** 1307–1311 (2011).
9. Seelig, G., Soloveichik, D., Zhang, D. Y. & Winfree, E. Enzyme-free nucleic acid logic circuits. *Science* **314,** 1585–1588 (2006).
10. Qian, L., Winfree, E. & Bruck, J. Neural network computation with DNA strand displacement cascades. *Nature* **475,** 368–372 (2011).
11. Weiner, L. M., Surana, R. & Wang, S. Monocolonal antibodies: versatile platforms for cancer immunotherapy. *Nature Rev. Immunol.* **10,** 317–327 (2010).
12. Grützkau, A. & Radbruch, A. Small but mighty: how the MACS-technology based on nanosized superparamagnetic particles has helped to analyze the immune system within the last 20 years. *Cytometry A* **77,** 643–647 (2010).
13. Ichise, M. & Harris, P. E. Imaging of β-cell mass and function. *J. Nucl. Med.* **51,** 1001–1004 (2010).
14. De Silva, A. P. & Uchiayam, S. Molecular logic and computing. *Nature Nanotech.* **2,** 399–410 (2007).
15. Katz, E. & Privman, V. Enzyme-based logic systems for information processing. *Chem. Soc. Rev.* **39,** 1835–1857 (2010).
16. Bendall, S. C. *et al.* Single-cell mass cytometry of differential immune and drug responses across a human hematopoietic continuum. *Science* **332,** 687–696 (2011).
17. Liu, H., Chumsae, C., Gaza-Bulseco, G., Hurkmans, K. & Radziejewski, C. H. Ranking the susceptibility of disulfide bonds in human IgG1 antibodies by reduction, differential alkylation, and LC-MS analysis. *Anal. Chem.* **82,** 5219–5226 (2010).
18. Holmes, D. Buy buy bispecific antibodies. *Nature Rev. Drug Discov.* **10,** 798–800 (2011).
19. Söderberg, O. *et al.* Direct observation of individual endogenous protein complexes *in situ* by proximity ligation. *Nature Methods* **3,** 995–1000 (2006).
20. Douglas, S. M., Bachelet, I. & Church, G. M. A logic-gated nanorobot for targeted transport of molecular payloads. *Science* **335,** 831–834 (2012).
21. Gu, H., Chao, J., Xiao, S.-J. & Seeman, N. C. A proximity-based programmable DNA nanoscale assembly line. *Nature* **465,** 202–205 (2010).

22. Lund, K. *et al.* Molecular robots guided by prescriptive landscapes. *Nature* **13,** 206–210 (2010).
23. Butler, Z. & Rizzi, A. in *Distributed and Cellular Robots* (Springer Handbook of Robotics, eds Siciliano, B. & Khatib, O.) Ch. 39, 911–920 (Springer, 2008).

Acknowledgements

The research presented in this manuscript, as well as past attempts that eventually led to the current design, was supported by the National Institutes of Health (R21CA128452, RC2CA147925, R21EB014477 and RGM104960, to S.R. and M.N.S.), the National Science Foundation (CCF-0218262, CCF-0621600, ECCS-1026591 and CBET-1033288), the National Aeronautics and Space Administration (NAS2-02039), and a fellowship from the Lymphoma and Leukemia Foundation (CPD Award) to M.N.S. The authors thank J. Loeb, E. Meffre and D. Stefanovic for their advice and comments on the manuscript.

Author contributions

M.R. and S.T. are considered equal first authors. M.R. was the principal experimenter on cells, and S.T. carried out conjugations and optimized cascades in the solution phase. P.P. performed exploratory experiments. A.D. and S.K. carried out model experiments on beads. S.R. was in charge of flow cytometry experiments, and S.T. and M.N.S. were in charge of non-cell-based experiments. M.N.S. and V.B. designed and suggested early proposals for the implementation of molecular computing on cell surfaces and settled on lymphocytes as targets. M.R., S.T., S.R. and M.N.S. analysed the data. S.R. and M.N.S. were the primary designers of the experiments and are most responsible for the structure of the presentation in this paper. M.N.S. wrote the initial draft of the manuscript.

Additional information

Supplementary information is available in the online version of the paper. Reprints and permissions information is available online at www.nature.com/reprints. Correspondence and requests for materials should be addressed to S.R. and M.N.S.

Competing financial interests

The authors declare no competing financial interests.